# Improvement in Performance of a Thermochemical Heat Storage System by Implementing an Internal Heat Recovery System


***Citation for published version (APA):***
Gaeini, M., Saris, L., Zondag, H. A., & Rindt, C. C. M. (2015). Improvement in Performance of a Thermochemical Heat Storage System by Implementing an Internal Heat Recovery System. In *Proceedings of The 13th International Conference on Energy Storage*

***Document status and date:***
Published: 01/05/2015

***Please check the document version of this publication:***

• A submitted manuscript is the version of the article upon submission and before peer-review. There can be important differences between the submitted version and the official published version of record. People interested in the research are advised to contact the author for the final version of the publication, or visit the DOI to the publisher's website.
• The final author version and the galley proof are versions of the publication after peer review.
• The final published version features the final layout of the paper including the volume, issue and page numbers.

Link to publication

*General rights*
Copyright and moral rights for the publications made accessible in the public portal are retained by the authors and/or other copyright owners and it is a condition of accessing publications that users recognise and abide by the legal requirements associated with these rights.

• Users may download and print one copy of any publication from the public portal for the purpose of private study or research.
• You may not further distribute the material or use it for any profit-making activity or commercial gain
• You may freely distribute the URL identifying the publication in the public portal.

If the publication is distributed under the terms of Article 25fa of the Dutch Copyright Act, indicated by the “Taverne” license above, please follow below link for the End User Agreement:

www.tue.nl/taverne

*Take down policy*
If you believe that this document breaches copyright please contact us at:

openaccess@tue.nl

providing details and we will investigate your claim.

Download date: 04. Oct. 2023

# Improvement in Performance of a Thermochemical Heat Storage System by Implementing an Internal Heat Recovery System

Mohammadreza Gaeini[1], Luuk Saris[1], Herbert A. Zondag[1, 2], Camilo C.M. Rindt[1,*]

[1] Eindhoven University of Technology, Department of Mechanical Engineering, P.O.Box 513, 5600 MB Eindhoven, The Netherlands.
[2] ECN, Energy Research Centre of the Netherlands, P.O. Box 1, 1755 ZG Petten, The Netherlands.

[*]*Corresponding email: C.C.M.Rindt@tue.nl*

*Keywords: Thermochemical seasonal heat storage, Built environment application, Domestic hot water, Heat recovery, Zeolite 13X*

## SUMMARY

A lab-scale prototype of a thermochemical heat storage system, employing a water-zeolite 13X as the working pair, is designed and optimized for providing hot tap water. During the hydration process, humid air is introduced to the packed bed reactor filled with dehydrated zeolite 13X, and the released heat of adsorption heats up the air passing through the reactor. The hot outflow air is led to an air-to-water heat exchanger integrated in a water tank and heats up the water. The residual heat in the exhaust air is used to preheat the reactor inflow in an air-to-air heat exchanger. The temperatures of all system components are measured, and the thermal powers and heat losses are calculated. Experiments are performed in the system with and without using the heat recovery, and improvement in performance of the heat storage system is investigated.

## INTRODUCTION

According to the International Energy Agency (IEA), the building sector is the largest consumer of energy and accounts for approximately 40% of the world's total primary energy consumption (Saheb 2011). Therefore, significant reductions in fossil fuel consumption are possible by using renewable energy sources in this sector. Solar energy is one of the most promising sustainable energy sources which can be used in order to reduce total energy consumption of a house, made possible by using new innovative solar energy technologies (Schnieders 2003).

Since both the solar irradiation and the energy demand in the built environment show large asynchronous variations during a year, in order to overcome the seasonal mismatch in the built environment applications, a long-term heat storage method is needed, which in comparison with the conventional heat storage methods has higher energy storage density and almost no heat loss (Hawes et al. 1993). By applying thermochemical heat storage, heat produced by solar collectors during summer can be stored in an endothermic dissociation reaction of a ThermoChemical Material (TCM), splitting it into two components (charging), and the energy stored in this way can be retrieved during winter by the reverse exothermal reaction between the components (discharging). A comparison between different materials is done by Shigeishi et al. 1979, showing that a candidate fulfilling these requirements is zeolite 13X which is non-toxic, non-corrosive and stable with high energy storage density. Although zeolite is relatively expensive, it is still a good candidate to be used in scientific studies because of its stability.

In literature, two types of sorption systems can be distinguished: open and closed systems. In an open system, an air stream is transporting water vapour and heat in and out of the packed bed of solid adsorbent; in a closed system on the other hand, no material is exchanged with the ambient but only energy. The MODESTORE project of the AEE/Intec is an example of a closed system. The system works with the water-silica gel pair and creates a temperature step of 10°C during hydration by dehydration at around 88°C (Jähnig et al. 2006). The Monosorp project conducted in ITW is an open sorption system with 8 $m^3$ of zeolite 4A designed for seasonal heat storage in a single-family passive house (N'Tsoukpoe 2009). During the regeneration phase, solar excess heat is used to dry the zeolite and charge the system and the exhaust air is used to preheat the inlet air. During the discharge period, humid indoor air is blown through the sorption bed and the released energy is transferred to the ventilation inflow air by a heat exchanger. An open adsorption system developed in ZAE Bayern is used as a buffer in a district heating network to store 1300 kWh for heating a school building during 14 hours with a maximum power of 135 kW (Hauer 2007). This system is charged in periods when energy is available from the net in off-peak hours. The system uses zeolite 13X as adsorbent and is connected to a district heating network.

At the Eindhoven University of Technology, an open atmospheric system with a packed bed reactor on lab-scale, using water-zeolite 13X as working pair was designed and tested in order to investigate the applicability of thermochemical heat storage for providing hot tap water in the built environment (Gaeini et al. 2014). However the water temperature of 60°C needed for hot tap water was not achieved. The purpose of the present work is to investigate the major losses in the system by measuring the temperatures of all system components and calculating the corresponding heat fluxes. By producing the complete thermal picture of the setup, the aim is to determine a way to yield hot tap water temperature. The performance of the system is studied experimentally and numerically, and is improved by implementing heat recovery and reducing the heat losses from the different components in the system.

## METHODS

### Experimental setup

In order to simulate the thermochemical heat storage system, a test setup is designed and tested. In Figure(1), a schematic view of the whole setup is shown. The sorption system is composed of five major components: the heat source (electrical heater), the humidifier bubble column, the heat exchanger, the sorption reactor for long term energy storage, and the water tank for short term energy storage. The complete cycle consists of two half cycles for dehydration and hydration, to store and regenerate thermal energy, respectively. The temperatures are measured in different places in the system during the dehydration and hydration processes as shown in Figure(1).

During dehydration, the compressed air flows into the system with a flow rate regulated by the Mass Flow Controller (MFC). The air is heated by the heater and goes into the reactor, where heat is transferred to the zeolite bed and drives the water desorption from the zeolite. The water vapor is blown out of the reactor by the air flow.

During the hydration, air is blown into the bubble column at the bottom, gets humid and exits the column from the top. The humid air flow blown off to the ambient until it gets steady, and then by flowing the prepared humid air to the reactor, exothermic sorption takes place in the reactor where water vapor is absorbed by the zeolite. The generated heat is transferred to the air and flows out of the reactor at the bottom. The heated air from the reactor flows to the water tank where the heat is transferred to the water by an integrated air-to-water heat exchanger inside the water tank. The exhaust air from the water tank flows into the air-to-air heat exchanger where the remaining heat of the air is used to preheat the inflow air to the reactor in order to reach higher temperatures.

The reactor is a cylindrical tank made of stainless steel. Cold humid or hot dry air flows into the reactor at the top and the hot dry air flows out at the bottom. The temperatures are measured at two different heights and two different radial positions in the bed, and at the inlet and outlet of the reactor. The water tank is also a 2 liters cylindrical tank made of stainless steel with an air-to-water heat exchanger mounted inside it, consisting of 61 vertical copper pipes. The heater has a power of 400 W and can be used during both dehydration in order to charge the material and during hydration in order to simulate an air-to-air heat exchanger with higher efficiency (compensating for losses in the real air-to-air heat exchanger). As humidifier, a bubble column filled with water is used, in which air is ingected at the bottom, and humid air exits at the top. The air-to-air heat exchanger, used to recover the heat from the outflow air of the system to preheat the inflow air to the system, is a cross flow heat exchanger made of aluminium. The inflow and outflow temperatures of both cold and hot sides of the heat exchanger are measured, to evaluate its effectiveness and efficiency. To minimize the heat losses, the whole system is insulated with 2cm layer of Armaflex HT. The whole setup is mounted on an aluminium frame. More details about the setup can be found in Gaeini et al. 2014.

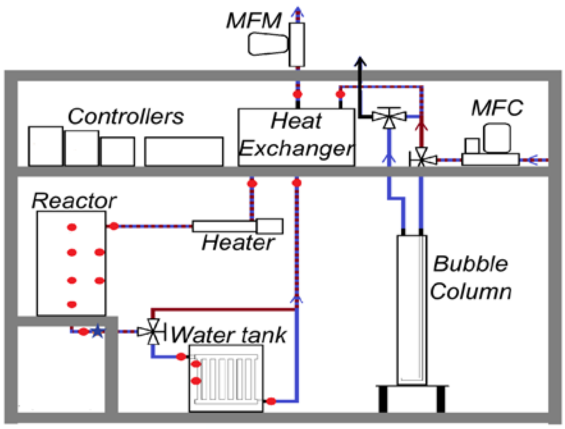


*Figure(1): Schematic illustration of the setup. The blue lines represent the hydration and the red lines represent the dehydration process paths. Red dots and blue star indicate the location of the thermocouples and the humidity sensor, respectievly.*

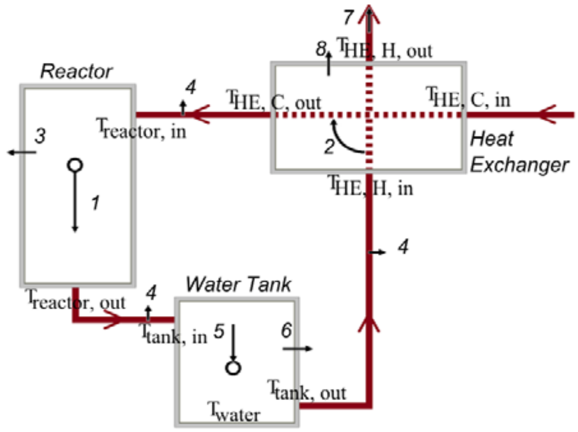


*Figure(2): Schematic illustration of the energy flows in the system during hydration; the black arrows indicate energy flows introduced in "Thermal analysis" section.*

**System model**

In order to perform a parameter study a model has been developed in Matlab for the hydration process. The system comprises of three main components (heat exchanger, reactor and water vessel) and the pipes in between as depicted in Figure(2).

The reactor is segmented along the height and for each time step equations (1) and (2), which express the energy balances for the gas and solid phases in the reactor, are solved. The energy balances in two phases are in connection with each other through the heat transfer term between the zeolite particles and the air, where $h_v$ is the volumetric heat transfer coefficient, and $T_a$ and $T_b$ are the air and bed temperatures, respectively. In equation(2) the left hand side term is for heat accumulation in both bed material and the wall of the reactor, where $A$ is the cross-sectional area of the bed and $\Delta x$ is the length of the segment. The second and third terms on the right hand side of equation(2) are the source terms related to the reaction energy and heat loss from the reactor.

$$\varepsilon\rho_a C_{P,a}\frac{\partial T_a}{\partial t} = -\frac{\dot{m}_a C_{P,a}}{A}\frac{\partial T_a}{\partial x} + h_v(T_b - T_a) \quad (1)$$

$$\left[(1-\varepsilon)\rho_b C_{P,\mathrm{b}} + \frac{m_r C_{P,r}}{A\Delta x}\right]\frac{\partial T_b}{\partial t} = -h_v(T_b - T_a) + \frac{\dot{r}\Delta H}{A\Delta x} - \frac{UA_{loss,reactor}}{A\Delta x}(T_b - T_{amb}) \quad (2)$$

The water tank is divided into segments in vertical direction and during the time equations (3) and (4), which represents the energy balances for the air flow inside the air-to-water heat exchanger integrated in the water tank and for the water inside the water tank, are solved. The thermal mass of the wall of the water vessel is taken into account in the total heat capacity of the tank, $m_t C_{P,\mathrm{t}}$.

$$-\dot{m}_a C_{P,\mathrm{a}}\frac{\partial T_a}{\partial x} = \frac{\mathrm{UA}_{HE,\tan k}}{L_{HE}}(T_a - T_w) \quad (3)$$

$$m_t C_{P,\mathrm{t}}\frac{\partial T_w}{\partial t} = \dot{m}_a C_{P,\mathrm{a}}(T_{a,in} - T_{a,out}) - \mathrm{UA}_{\mathrm{loss},\tan k}(T_w - T_{amb}) \quad (4)$$

In order to consider the heat loss from the heat exchanger and the heat accumulation in the body of the heat exchanger, the temperature of the air-to-air heat exchanger, $T_{HE}$, is modeled by equation(5). The left hand side of the equation represents the heat accumulation in the body of the heat exchanger, where $m_{HE}$ and $C_{P,HE}$ are the mass and heat capacity of the body of the heat exchanger. The first two terms on the right hand side represent the energy transfer by the air flow at the hot and cold side of the heat exchanger, respectively. Where $\dot{m}_a$ and $C_{P,a}$ are the mass flow rate and heat capacity of the air. The last term represents the heat loss from the heat exchanger by its overall heat transfer coefficient, $\mathrm{UA}_{\mathrm{loss},HE}$, to the ambient at temperature $T_{amb}$. The outflow temperatures of the hot and cold sides ($T_{HE,h,out}$ and $T_{HE,c,out}$) are calculated based on the efficiency of the heat exchanger that is defined as heat flux by cold side air flow over maximum possible heat flux ($(T_{HE,\mathrm{C},out} - T_{HE,c,in})/(T_{HE,\mathrm{H,in}} - T_{HE,c,in})$). Heat losses in the pipes are considered by equation(7).

$$m_{HE} C_{P,HE}\frac{\partial T_{HE}}{\partial t} = \dot{m}_a C_{P,a}(T_{HE,\mathrm{H},out} - T_{HE,h,in}) - \dot{m}_a C_{P,a}(T_{HE,\mathrm{C},out} - T_{HE,c,in}) - \mathrm{UA}_{\mathrm{loss},HE}(T_{HE} - T_{amb}) \quad (5)$$

$$\dot{m}_a C_{P,a}\frac{\partial T_a}{\partial x} = \frac{UA_{loss,pipe}}{L_{pipe}}(T_a - T_{amb}) \quad (6)$$

**Thermal analysis**

In order to determine the total efficiency of the system, an energy balance is set by calculating the different energy contributions for all parts of the system, based on the numerically calculated and experimentally measured temperatures. Figure(2) shows a schematic view of the energy flows that are taken into account. The total energies are calculated from the start of the hydration ($t_s$), which is the time that the humid air is fed to the reactor, until the time when the total zeolite bed is reacted ($t_e$). Reactor energy is a combination of the reaction energy produced in the reactor and the energy losses from the reactor (two first terms in the list) and can be calculated by equation(8). The fourth term in the list, the energy losses from the pipes, is the summation of the losses in the three main pipes between the three main components of the system. The heat loss in each pipe is calculated by equation(10). The energy flows are listed below and can be calculated by the following equations:

1. Reaction energy ($E_{reaction}$)
2. Energy losses through the wall of the reactor ($E_{loss,reactor}$)
3. Recovered heat by the heat exchanger ($E_{recovered}$)
4. Energy losses from the pipes ($E_{loss,pipe}$)
5. Energy used to heat up the water ($E_{water}$)
6. Energy losses from the water tank ($E_{loss,tank}$)
7. Energy losses from the outflow air ($E_{loss,out}$)
8. Energy losses through the wall of the heat exchanger ($E_{\mathrm{loss,HE}}$)

$$E_{reactor} = E_{reaction} - E_{loss,reactor} = \sum_{t_s}^{t_e} \dot{m}_a C_{P,a} (\mathrm{T}_{reactor,out}(t) - T_{reactor,in}(t))\Delta t \tag{7}$$

$$E_{recovered} = \sum_{t_s}^{t_e} \dot{m}_a C_{P,a} (T_{HE,C,in}(t) - \mathrm{T}_{HE,C,out}(t))\Delta t \tag{8}$$

$$E_{loss,pipe} = \sum_{t_s}^{t_e} \dot{m}_a C_{P,a} (\mathrm{T}_{pipe,out}(t) - T_{pipe,in}(t))\Delta t \tag{9}$$

$$E_{water} = m_w C_{P,w} (\mathrm{T}_w(\mathrm{t}_e) - T(t_s)) \tag{10}$$

$$E_{loss,tank} = \left[ \sum_{t_s}^{t_e} \dot{m}_a C_{P,a} (\mathrm{T}_{tank,out}(t) - T_{tank,in}(t))\Delta t \right] - E_{water} \tag{11}$$

$$E_{loss,out} = \sum_{t_s}^{t_e} \dot{m}_a C_{P,a} (\mathrm{T}_{HE,H,out}(t) - T_{HE,C,in}(t))\Delta t \tag{12}$$

$$E_{\mathrm{loss,HE}} = \sum_{t_s}^{t_e} \dot{m}_a C_{P,a} (T_{HE,\mathrm{H},in}(t) - \mathrm{T}_{HE,\mathrm{H},out}(t) + T_{HE,\mathrm{C},in}(t) - T_{HE,\mathrm{C,out}}(t))\Delta t \tag{13}$$

## RESULTS

### Model validation

The numerical results are compared with the results of one hydration experiment with an air flow rate of 70 l/min. The temperatures calculated by the model are compared with the measured ones in Figure(3). The energy balances based on the numerically calculated temperatures and on the experimentally measured temperatures for the hydration experiment are compared in Table (1). The comparisons for both temperature profile and energy balance show a good agreement between numerical and experimental results. However, the experimental energy balance can not be as detailed as the one calculated by the model. For instance, $E_{reactor}$ is a combination of the reaction energy produced by the adsorption, the sensible heat in the reactor and the heat loss from the reactor. A more detailed thermal analysis is done based on the results of the model.

As can be seen in Table(1), the largest losses are the $E_{loss,tank}$ and $E_{loss,out}$. The heat loss in the water tank is a combination of the heat loss through the wall of the tank and the sensible heat adsorbed by the wall of the tank. The former one can be reduced by increasing the thickness of the insulation layer and the latter one can be reduced by decreasing the thermal mass of the body of water tank. In order to reduce the heat wasted to the ambient by the outflow air ($E_{loss,out}$), the efficiency of the heat exchanger should be increased. Effects of these adjustments on the thermal performance of the system are investigated in a parameter study in the next section.

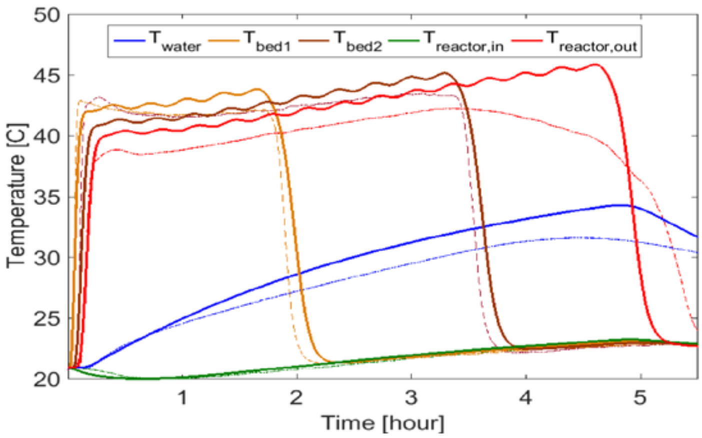


*Figure(3): Comparison between temperature profiles calculated by the model and measured ones*

*Table(1): Energies for the hydration in kJ.*

| terms | Exp. | Num. |
|---|---|---|
| $E_{reactor}$ | 393 | 413 |
| $E_{recovered}$ | 143 | 133 |
| $E_{loss,pipes}$ | 57 | 37 |
| $E_{water}$ | 81 | 107 |
| $E_{loss,tank}$ | 102 | 122 |
| $E_{loss,out}$ | 139 | 133 |
| $E_{loss,HE}$ | 14 | 14 |

### Parameter study

The validated model is employed to get more insight into the effect of parameter variations on the efficiency of the system. Parameter study is done for six cases (Table(2)) to find the best way to improve the system efficiency. The total efficiency of the system is defined as the energy heating up the water divided by the energy generated by the reactor ($\eta=E_{water}/E_{reaction}$). The major energy losses in the system, which are the outflow losses and the losses of the water tank, are varied to investigate the effects of heat exchanger efficiency and thermal mass of the water tank. The efficiency of the heat exchanger is increased to 90% and 100% in case 3 and case 4, respectively. In case 5, the thermal mass of the water tank is decreased from 7 to 5kJ/K. In case 6, which is a combination of cases 3 and 5, the efficiency of the system is increased by around 10% and 8% compared with case 1 (system without heat recovery) and case 2 (system with the existing heat recovery), respectively.

*Table(2): Effects of different parameters on thermal performance of the system.*

| cases | Recovered energy | Water temperature | Efficiency |
|---|---|---|---|
| 1. Without the heat exchanger | 0 kJ | 34.1°C | 19.2% |
| 2. With the heat exchanger (efficiency=40%) | 69 kJ | 35.8°C | 21.6% |
| 3. Increased heat exchanger efficiency to 90% | 187 kJ | 38.6°C | 25.5% |
| 4. Increased heat exchanger efficiency to 100% | 222 kJ | 39.8°C | 27.1% |
| 5. Decreased thermal mass of water tank | 91 kJ | 37.5°C | 24.0% |
| 6. Combined improvements 3 and 5 | 254 kJ | 41.8°C | 29.9% |

The complete energy maps for six cases are shown in Figure (4). As can be seen, by improving the heat exchanger efficiency and decreasing the thermal mass of the water tank, the losses related to the outflow air and adsorbed heat by the body of the water tank are significantly decreased in case 6. In case 6, the largest share of the losses are related to the heat losses through the walls of the reactor, water tank and pipes; which suggest that increasing the thickness of the insulation is needed in the whole system. These adjustments are included in the system configuration in the discussion.

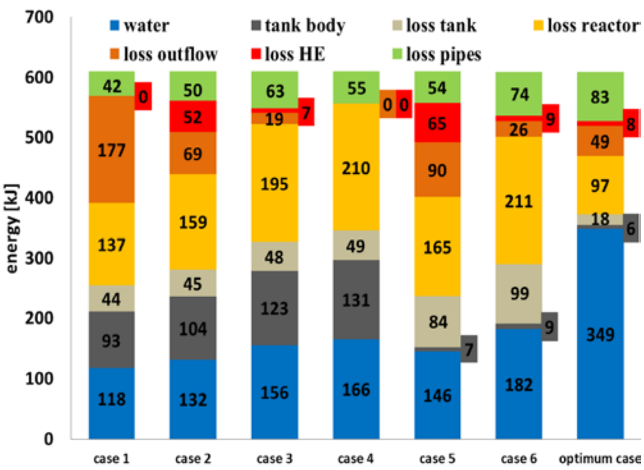


*Figure(4): Energy maps calculated by the model for the different cases.*

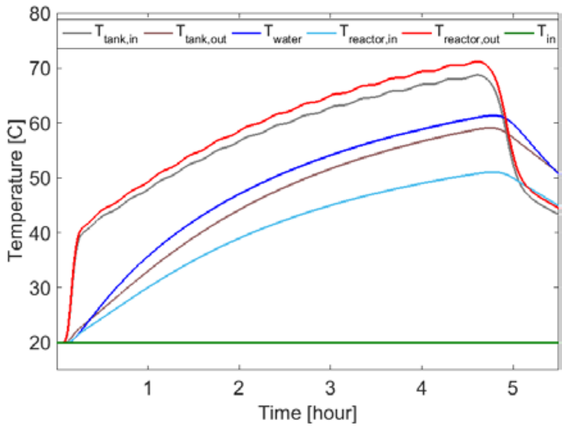


*Figure(5): Temperature profile for optimum case calculated by the model.*

**DISCUSSION**

The parameter study shows that the improvement of the air-to-air heat exchanger efficiency and the decrease of the water tank thermal mass improve the water temperature. However, in order to reach the required hot tap water temperature, other adjustments are required. The following measures are taken as further adjustments in the model to achieve water temperature of 60°C: (1) an increased air-to-air heat exchanger efficiency to 90%; (2) a decreased thermal mass of the water tank to 0.5kJ/K; (3) an increased insulation thickness with a factor 5. The temperature profile is shown in Figure(5) and the corresponding energy map is represented as optimum case in Figure(4). In this case the system efficiency is improved to 57%.

## CONCLUSIONS

Numerical and experimental investigations are done on a thermochemical lab-scale heat storage system, for providing hot tap water. The numerical model is validated by comparison between numerical results and experimental results. First the numerically calculated temperatures in the system are compared with experimental ones. Further the energy balance is determined from the numerical temperatures and is compared with the energy balance calculated from experiment. The validated model is used to get more detailed information about the energy map of the system. A parameter study is done by the model to investigate effects of the heat recovery, the thermal mass of the water tank, and the insulation thickness. The heat recovery can improve the efficiency of the system by around 8% compared with the system without heat recovery. Decreasing the thermal mass of the water tank can improve the efficiency by 2.5%. Since the improvement in the efficiency of the system leads to higher temperatures in all parts of the system, the heat losses through the walls of the system will increased. By improving the insulation of the system, the water temperature of 60°C is achieved. Based on the complete energy map several adjustments are suggested to improve the performance of the system.

## REFERENCES


Gaeini, M., Jong, D. E., Zondag, H. A., & Rindt, C. C. M., “Design of a thermochemical heat storage system for tap water heating in the built environment,” Proc. of the Eurotherm Seminar #99 Advances in Thermal Energy Storage (2014).

Hauer, A. "Adsorption Systems for TES-Design and Demonstration Projects," Thermal energy storage for sustainable energy consumption, pp. 409-427. Springer Netherlands, (2007).

Hawes, D., Feldman, D., and Banu, D., “Latent heat storage in building materials,” Energy and Buildings, 20(1), pp. 77–86, (1993).

Jähnig, D., Hausner, R., Wagner, W., and Isaksson, C., “Thermo-chemical storage for solar space heating in a single-family house,” Proc. of ecostock. New Jersey (2006).

N’Tsoukpoe, K. E., Liu, H., Le Pierrès, N., & Luo, L., “A review on long-term sorption solar energy storage,” Renewable and Sustainable Energy Reviews, 13(9), pp. 2385-2396, (2009).

Saheb, Y., “Modernising building energy codes to secure our global energy future,” The IEA Policy Pathway series, (2011).

Schnieders, J., “Cepheus–measurement results from more than 100 dwelling units in passive houses,” European Council for an Energy Efficient Economy: Summer Study, (2003).

Shigeishi, R. A., Langford, C. H., and Hollebone, B. R., “Solar energy storage using chemical potential changes associated with drying of zeolites,” Solar Energy, 23(6), pp. 489-495, (1979)